

# Standing on the Shoulders of Giants: Reprogramming Visual-Language Model for General Deepfake Detection

Kaiqing Lin<sup>1</sup>, Yuzhen Lin<sup>1</sup>, Weixiang Li<sup>1</sup>, Taiping Yao<sup>2</sup>, Bin Li<sup>1</sup>

<sup>1</sup>Guangdong Provincial Key Laboratory of Intelligent Information Processing, Shenzhen Key Laboratory of Media Security, SZU-AFS Joint Innovation Center for AI Technology, Shenzhen University

<sup>2</sup>Tencent YouTu Lab

## Abstract

The proliferation of deepfake faces poses huge potential negative impacts on our daily lives. Despite substantial advancements in deepfake detection over these years, the generalizability of existing methods against forgeries from unseen datasets or created by emerging generative models remains constrained. In this paper, inspired by the zero-shot advantages of Vision-Language Models (VLMs), we propose a novel approach that repurposes a well-trained VLM for general deepfake detection. Motivated by the model reprogramming paradigm that manipulates the model prediction via data perturbations, our method can reprogram a pre-trained VLM model (e.g., CLIP) solely based on manipulating its input without tuning the inner parameters. Furthermore, we insert a "pseudo-word" guided by facial identity into the text prompt. Extensive experiments on several popular benchmarks demonstrate that (1) the cross-dataset and cross-manipulation performances of deepfake detection can be significantly and consistently improved (e.g., over 88% AUC in cross-dataset setting from FF++ to WildDeepfake) using a pre-trained CLIP model with our proposed reprogramming method; (2) our superior performances are at less cost of trainable parameters, making it a promising approach for real-world applications.

## Introduction

Deepfake refers to a series of deep learning-based facial forgery techniques (Li et al. 2020a; Yao et al. 2021; Xu et al. 2022; Chen et al. 2024) that can swap or reenact the face of one person in a video to another. In recent years, deepfake videos (a.k.a, deepfakes) have gained substantial attention due to their potential by creating and spreading false information. Thus, detecting deepfakes has emerged as a crucial research topic to reduce such security risks.

Existing methods treat deepfake detection as a binary classification problem and predominantly utilize CNNs (e.g., Xception (Chollet 2017) or EfficientNet (Tan and Le 2019)) as the backbones of classifier. In addition, some works (Qian et al. 2020; Li et al. 2020b; Zhao et al. 2021; Liu et al. 2021) propose to introduce auxiliary clues, including modalities (e.g., frequency) or supervision (e.g., forgery masks) information for learning subtle forgery artifacts. Despite these advancements, evaluating forgeries from unseen datasets and synthesized by unseen methods beyond the

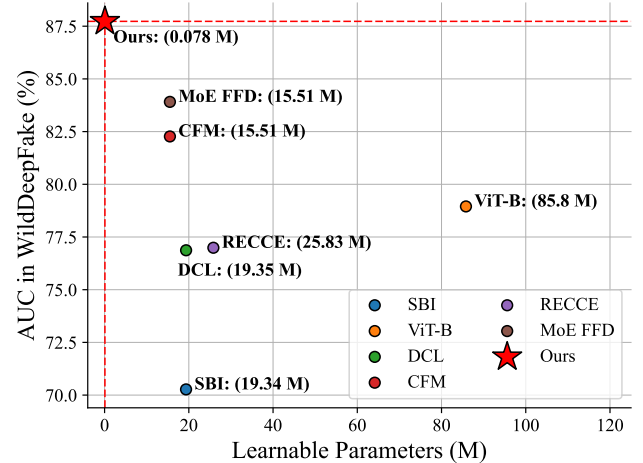


Figure 1: Comparison between our method and open-source deepfake detection models on the WildDeepfake dataset (trained on FF++). Our method with the fewest learnable parameters while achieves the best performance.

training data still poses a significant challenge for practical deepfake detection.

To enhance the generalizability of deepfake detectors, several works employ vision transformer (ViT) (Dosovitskiy et al. 2021) models as the backbone, owing to their superior image representation capabilities compared to CNNs. Nevertheless, ViT-based detection methods, e.g. UiA-ViT (Zhuang et al. 2022) and Bi-LIG (Jiang et al. 2024), typically involve fully fine-tuning pre-trained ViT-based backbones (e.g., with ImageNet weights). This process demands extensive computational and storage resources, which hinders their practical deployment in real-world applications. Thus, developing a general yet cost-efficient approach is necessary for deepfake detection.

Due to the inherent vulnerability of deep networks to adversarial attacks, a novel concept called model reprogramming (Elsayed, Goodfellow, and Sohl-Dickstein 2019; Chen 2024) has been proposed to re-purpose a well-trained model trained in a source domain to perform a target-domain task through learning a universal perturbation without modifying the source-domain model parameters. In other words, an ad-

ditive offset applied to a deep network’s input would be sufficient to adapt the network to a new task without the need of re-training or fine-tuning its inner parameters. It is evident that the reprogramming paradigm requires significantly fewer computing resources compared to fine-tuning numerous parameters within the model. Inspired by the above advancements, we advocate that reprogramming a well-trained foundation model to identify deepfakes is a promising way in terms of computational efficiency. Considering the Vision Language Models (VLMs) (Bordes et al. 2024) have shown impressive zero-shot performances by bridging vision and language modalities, we employ CLIP (Radford et al. 2021) as the foundation model and adapt it to identify deepfakes.

To this end, in this paper, we propose RepDFD, a novel method to reprogram a pre-trained CLIP model for effective and general deepfake detection. RepDFD solely learns single perturbations in pixel spaces for the deepfake detection task while keeping the entire CLIP model frozen. Specifically, we introduce *Input Transformation* to merge the image and learnable perturbations and then feed it into the image encoder of CLIP. Furthermore, we propose *Face2Text Prompts* to generate text prompts merging facial identity information, and then feed them into the text encoder of CLIP to guide the optimization of perturbations. During the testing phase, the sole operation involves adding such task-specific perturbations (a.k.a, visual prompts) to all test images before feeding them into the CLIP model for evaluation. This straightforward method enables the CLIP model to effectively detect deepfakes. Moreover, since the internal parameters are not trained, the foundation CLIP model can be reused for the other vision tasks. Extensive experiments on several popular deepfake benchmarks demonstrate that (1) the cross-dataset and cross-manipulation performances can be significantly and consistently enhanced by equipping RepDFD for a pre-trained CLIP model; and (2) our superior performances are at less cost of trainable parameters (See in Figure 1), making it a promising approach for real-world applications.

Briefly, the main contributions of this work can be summarized as follows:

- This is the first work to explore utilizing the model reprogramming paradigm for deepfake detection.
- We propose novel RepDFD to reprogram a pre-trained CLIP model by solely processing its image and text inputting without tuning the inner parameters. Thus, RepDFD can be seamlessly adapted to other foundation models in a plug-and-play way.
- We conduct extensive experiments on several benchmarks, and demonstrate that RepDFD is general and efficiency for deepfake detection.

## Related Works

### Deepfake Detection

The past five years have witnessed a wide variety of methods proposed for defending against the malicious usage of deepfakes. Currently, the majority of deepfake detection methods are based on deep learning, leveraging generic CNNs (e.g.,

Xception(Chollet 2017), EfficientNet(Tan and Le 2019)) as the backbones of the classifier. Furthermore, several works (Qian et al. 2020; Liu et al. 2021; Zhao et al. 2021) utilize frequency information or localize the forged regions to improve the performance of detectors. Nevertheless, the generalization challenge still hinders the application of deepfake detectors in real-world scenarios. To address such issue, several works (Li et al. 2020b; Shiohara and Yamasaki 2022; Larue et al. 2023; Nguyen et al. 2024) introduce the pseudo deepfake data, which blending two different faces, during the training. However, all of the above methods typically involve retraining at least one backbone network. In general, employing more powerful backbone networks (e.g., replacing CNNs with ViTs) produces better performances but at the cost of increased computational resources.

### CLIP Model

CLIP is a vision-language model (Radford et al. 2021), that is able to perform flexible zero-shot transfer to unseen classes using text prompts. Since CLIP is pre-trained to predict whether an image matches a textual description, it naturally fits zero-shot recognition. This is achieved by comparing image features with the classification weights synthesized by the text encoder, which takes as input textual descriptions specifying classes of interest. The CLIP model contains an image-encoder  $E_I(\cdot)$  and a text-encoder  $E_T(\cdot)$  such that the cosine similarity between the features  $E_I(x_k)$  and  $E_T(t_k)$  are maximized with respect to each pair  $k$ . Compared with the traditional classifier learning approach where closed-set visual concepts are learned from random vectors, vision-language pre-training allows open-set visual concepts to be explored through a high-capacity text encoder, leading to a broader semantic space and in turn making the learned representations more transferable to various vision tasks. Several works(Sha et al. 2023; Ojha, Li, and Lee 2023; Cozzolino et al. 2024) has explore that using CLIP model for detecting generated image by GANs and Diffusion Models. VLFFD proposes to fully fine-tune CLIP with fine-grained text prompts for deepfake detection. In this work, we propose a cost-efficient method to adapt a large pre-trained CLIP model for general deepfake detection.

### Parameter-Efficient Tuning

Parameter Efficient Fine-Tuning (PEFT) methods, which significantly reduce computational and storage overheads, have garnered increasing attention. By fine-tuning only a limited number of additional parameters, PEFT can adapt a large pretrained model to achieve outstanding performance in targeted tasks.

One of the PEFT methods, Model Reprogramming (Chen 2024), which incorporates prompts into inputs, offers an effective framework for repurposing models for various task-specific applications. The framework draws significant inspiration from adversarial reprogramming, which was first introduced by Elsayed et al (Elsayed, Goodfellow, and Sohl-Dickstein 2019) The aim of model reprogramming is to re-use and re-align the data representation, from an existing model, for a separate task without fundamental changes

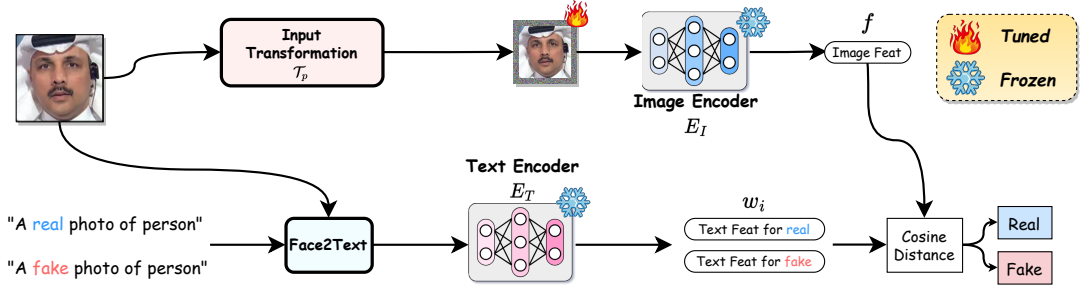


Figure 2: Overall framework of our proposed method. The core idea involves optimizing an universal visual prompt on a frozen CLIP model to adapt it for the deepfake detection task.

to the model’s parameters. This paradigm re-purposes existing knowledge by strategically transforming inputs and outputs, bypassing extensive inner model parameter fine-tuning. Reprogramming techniques have been widely applied in various tasks in the past few years. VP introduces a universal perturbation directly into the input data to facilitate task-specific fine-tuning while keeping the pretrained model intact. Although these PEFT methods have developed in other research fields, the application of PEFT methods to face forgery detection remains largely unexplored. In this study, we introduce a novel approach to reprogramming a pre-trained CLIP model for deepfake detection using a minimal number of learnable parameters, designed to leverage the great generalization abilities of the pretrained Vision-Language Model (VLM).

## Methodology

### Overview

The goal of our method is to adapt the frozen CLIP model for deepfake detection task by solely learning a single visual prompt. Formally, given a well-trained CLIP model (including the image encoder  $E_I(\cdot)$  and the text encoder  $E_T(\cdot)$ ), we learn a single visual prompt  $\delta$  for adapting the frozen  $E_I(\cdot)$  and  $E_T(\cdot)$  to identify deepfakes. To achieve this, we propose *Input Transformation* and *Face2Text Prompts*, which solely process the image and text before inputting  $E_I(\cdot)$  and  $E_T(\cdot)$ , respectively. During evaluation, the optimized  $\delta$  is added to the input images to enhance the visual clues of identifying deepfakes. In this way, we harness the power of learned perturbations to guide the CLIP model to focus the deepfake detection task while preserving its inner parameters. The overall framework is depicted in Figure 2. In what follows, we elaborate on the details of *Input Transformation*, *Face2Text Prompts* and the optimization pipeline.

### Input Transformation

In designing the placement of visual prompts, we adopt a similar scheme to (Bahng et al. 2022; Tsao et al. 2024), wherein visual prompts are placed around images for input transformations. Although the input image size is determined by the source model, when fine-tuning to a downstream dataset from a source model, there is design freedom to resize the target images and use the remaining space for

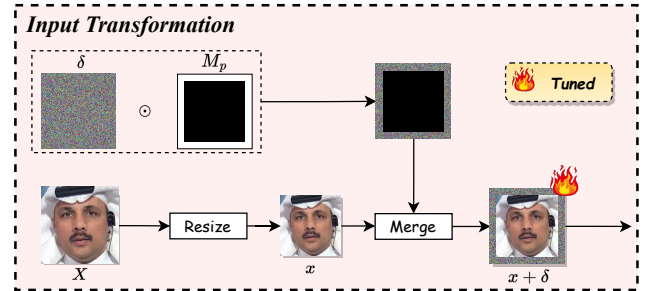


Figure 3: Illustration of Input Transformation

visual prompts. Figure 3 demonstrates the details of Input Transformation. Given an original image  $X$ , the input transformation aims to merge the universal perturbation  $\delta$  to  $X$ . Mathematically, we describe the process of input transformations as

$$\mathcal{T}_p(\mathbf{X}, \delta) = \text{Resize}_p(\mathbf{X}) + \mathbf{M}_p \odot \delta \quad (1)$$

where  $p$  is the width of the visual prompt and  $M_p$  is a binary mask with a border of width  $p$ . The original image  $X$  of size  $H \times W$  is resized to  $H' \times W' = (H - 2p)(W - 2p)$ , so that the prompted image is of the same size as the original without overlapping with  $\delta$ . Note that the number of trainable parameters in our method is model-agnostic, which can be computed by

$$\#Para = 3(HW - H'W') = 6p(H + W) - 12p^2 \quad (2)$$

This expression indicates that  $\delta$  is applied to the RGB channels of the image.

We feed  $\mathcal{T}_p(\mathbf{X}, \delta)$  into image encoder to get the image feature  $f$ , i.e.,

$$f = E_I(\mathcal{T}_p(\mathbf{X}, \delta)) \quad (3)$$

### Face2Text Prompts

To map model outputs to the target label, the CLIP model utilizes text prompts to align image features in a shared latent space, enabling classification by matching the closest text description to the image features. For instance, one of the official unified templates of text prompts is “A photo of a [cls]”, where [cls] is a placeholder of class label. In the context of deepfake detection, the binary class labels “real face”

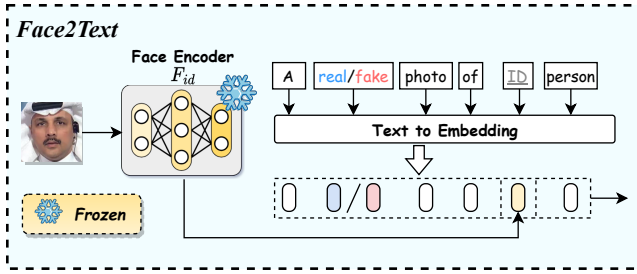


Figure 4: Illustration of Face2Text Prompts.

and “fake face” (or synonymous terms) lack specificity compared to labels such as “cat” or “dog”, making them difficult to accurately identify using existing text templates. To address this issue, VLFFD (Sun et al. 2023) proposes to introduce of fine-grained text descriptions manually to fine-tune both  $E_I(\cdot)$  and  $E_T(\cdot)$  in the CLIP model. However, designing a hand-crafted text prompt that comprehensively describes forgery clues is difficult and labor-intensive.

In this work, we aim to design simple yet effective text prompts to fully harness the generalizable capabilities of the CLIP model for deepfake detection. The success of personalized image generation methods has shown that introducing pre-trained image embedding as textual embeddings is beneficial for maintaining the consistency of generated subjects. Considering that deepfakes involve the manipulation of faces, the inconsistency of facial representations between real and fake faces is a reliable clue. Inspired by this, we suggest exploit the CLIP text encoder to integrate face embeddings into text embeddings. Therefore, the face information, which is difficultly expressed by language, can be incorporated into textual prompts, thereby enhancing the CLIP model’s capability for efficient deepfake detection.

To achieve this, a Face2Text module is proposed and the details are shown in Figure 4. The prompt template is designed as “A [cls] photo of a [ID] person”. Given a face encoder  $F_{id}$ , we represent a face embedding  $S^*$  for an input image  $\mathbf{X}$ :

$$S^* = f_{\text{map}}(F_{id}(\mathbf{X})). \quad (4)$$

Following tokenization, we substitute the placeholder token [ID] with the face embedding  $S^*$ , yielding a sequence of token.  $f_{\text{map}}$  represent a random projection layer to align the dimension. Herein, we employ a pre-trained Transface (Dan et al. 2023) as  $F_{id}$ .

We also consider the plain text template that “A [cls] photo of a person”. Thus, we get four different text template for real and fake labels (See in Table1) One of interesting finding according to results the is that the class-specific setting  $\mathbf{T} = \{T_0, T_3\}$  achieves the best performance. The in-depth analysis are discussion later.

We feed tokenized  $\mathbf{T}$  into text encoder to get the text feature  $w$ , i.e.,

$$w = E_T(\text{ToEmbedding}(\mathbf{T})), \quad (5)$$

where the operation  $\text{ToEmbedding}$  represents the process of transforming words into word embeddings.

| Index | Textual Template              |
|-------|-------------------------------|
| $T_0$ | “A real photo of person”      |
| $T_1$ | “A fake photo of person”      |
| $T_2$ | “A real photo of [ID] person” |
| $T_3$ | “A fake photo of [ID] person” |

Table 1: Candidate templates of text prompts.

## Optimization Pipeline

Following the paradigm of CLIP, the prediction probability are calculated as,

$$P(y = i | x) = \frac{\exp(\cos(w_i, f)/\tau)}{\sum_{j=1}^2 \exp(\cos(w_j, f)/\tau)}, \quad (6)$$

where  $\cos(\cdot)$  denotes the cosine similarity and  $\tau$  is the temperature parameter of CLIP. Eq. (6) have consistent formulation to a traditional full connected layer with input dimension  $N$  and output dimension 2 if we treat the  $[w_r, w_f]$  as the ‘weight’ of a full connected layer.

During training we optimize the prompt by maximizing the likelihood of the correct label, and during inference we pad the optimized prompt around the shrunk test samples for predictions. For a training dataset  $\mathcal{D}$ , the optimization target can be formulated as minimizing  $\mathcal{L}$  as

$$\mathcal{L} = \mathbb{E}_{\mathbf{X} \sim \mathcal{D}} \left[ - \sum_i^N P(y_i|x) \log(P(y_i|x)) \right], \quad (7)$$

We initialize the  $\delta$  to zero, and follow a simple gradient-based approach to directly optimize the visual prompt via back-propagation which updates  $\delta$  at step  $t$  by

$$\delta^{t+1} = \delta^t - \gamma \nabla_{\delta^t} \mathcal{L}, \quad (8)$$

where  $\gamma$  is the learning rate.

## Experiments

### Experimental Settings

**Datasets** Following most previous works, we mainly conducted experiments on the FaceForensics++ (FF++) (Rossler et al. 2019). It contains 1000 Pristine (PT) videos (i.e., the real sample) and 5000 fake videos forged by five manipulation methods, i.e., Deepfakes (DF), Face2Face (F2F), FaceSwap (FS), NeuralTextures (NT) and FaceShifter (FSh). Besides, FF++ provides three quality levels in compression for these videos: raw, high-quality (HQ) and low-quality (LQ). The **HQ version of FF++** is adopted by default in this paper. The samples were split into disjoint training, validation, and testing sets at the video level follows the official protocol.

To demonstrate the performances in cross-dataset settings, four additional datasets are adopted, i.e., Celeb-DF-v2 (CDF) (Li et al. 2020c), DeepFake Detection Challenge preview (DFDCP) (Dolhansky et al. 2019), DeepFake Detection Challenge public (DFDC) (Dolhansky et al. 2020) and WildDeepfake (Wild) (Zi et al. 2020). See the supplementary material for more details.

| Method                | Frame-level  |              |              |              | Method              | Video-level  |              |              |              |
|-----------------------|--------------|--------------|--------------|--------------|---------------------|--------------|--------------|--------------|--------------|
|                       | CDF          | Wild         | DFDCP        | DFDC         |                     | CDF          | Wild         | DFDCP        | DFDC         |
| UIA-ViT (ECCV 2022)   | 82.41        | -            | 75.80        | -            | DCL (AAAI 2022)     | 82.30        | 71.14        | -            | 76.71        |
| CFM (TIFS 2024)       | 82.78        | 78.39        | -            | 75.82        | AUNet (CVPR 2023)   | 92.77        | -            | 86.16        | 73.82        |
| SLADD (CVPR 2022)     | 79.70        | -            | -            | 77.20        | SBI (CVPR 2022)     | 93.18        | -            | 86.15        | 72.42        |
| FoCus (TIFS 2024)     | 76.13        | 73.31        | 76.62        | 68.42        | TALL (ICCV 2023)    | 90.79        | -            | -            | 76.78        |
| UCF (ICCV 2023)       | 75.27        | -            | 75.94        | 71.91        | TALL++ (IJCV 2024)  | 91.96        | -            | -            | 78.51        |
| Ba et al. (AAAI 2024) | <b>86.40</b> | -            | 85.10        | 72.10        | SeeABLE (ICCV 2023) | 87.30        | -            | 86.30        | 75.90        |
| LSDA (CVPR 2024)      | 83.00        | -            | 81.50        | 73.60        | LAA-Net (CVPR 2024) | <b>95.40</b> | 80.03        | 86.94        | -            |
| VLFFD (arXiv 2023)    | 84.80        | 83.55        | 84.74        | -            | IID (CVPR 2023)     | 83.80        | -            | -            | 81.23        |
| SA3WT (IJCV 2024)     | 83.80        | -            | -            | 76.02        | Bi-LIG (TIFS 2024)  | 97.93        | 83.00        | 91.24        | <b>82.57</b> |
| <b>Ours (DF)</b>      | 78.61        | <b>86.60</b> | 86.15        | 76.32        | <b>Ours (DF)</b>    | 88.41        | 87.73        | 90.68        | 80.53        |
| <b>Ours (FF++)</b>    | 80.00        | 85.42        | <b>90.57</b> | <b>77.34</b> | <b>Ours (FF++)</b>  | 89.94        | <b>88.05</b> | <b>95.03</b> | 80.99        |

Table 2: AUC(%) of cross-datasets evaluations. The results of other SOTA methods are directly cited from their corresponding original paper. The best results are highlighted.

| Training Data | Method      | DF           | FS           | FSh          |
|---------------|-------------|--------------|--------------|--------------|
| DF            | DCL         | 99.98        | 61.01        | 68.45        |
|               | IID         | 99.51        | 63.83        | 73.49        |
|               | <b>Ours</b> | 99.36        | <b>94.94</b> | <b>81.51</b> |
| FS            | DCL         | 74.80        | 99.90        | 64.86        |
|               | IID         | 75.39        | 99.73        | 66.18        |
|               | <b>Ours</b> | <b>98.31</b> | 99.59        | <b>85.21</b> |
| FSh           | DCL         | 63.98        | 58.43        | 99.49        |
|               | IID         | 65.42        | 59.50        | 99.50        |
|               | <b>Ours</b> | <b>89.99</b> | <b>81.22</b> | 99.82        |

Table 3: AUC(%) on cross-manipulation evaluations. The best cross-manipulation results are highlighted.

**Implementation details** We employ CLIP-ViT-L (Radford et al. 2021) as the foundation model, which is pretrained on LAION-400M. The input size of foundation model is  $224 \times 224$ , we set  $p = 34$  for Input Transformations, so that trainable parameters of our method is 0.078M, which can be computed by Equation 2. We employed the AdamW optimizer with the learning rate 1.0, and the weight decay was fixed at 0. Besides, the data preprocessing transform is as same as the original CLIP(Radford et al. 2021) At last, the visual prompt  $\delta$  is initialized by zero padding.

**Evaluation metrics** In this work, we mainly report the area under the ROC curve (AUC) to compare with prior works. The video-level results are obtained by averaging predictions over each frame on an evaluated video.

### Comparisons with State-of-the-Arts

To comprehensively evaluate the generalizability of our method, we compare the performances of cross-datasets and cross-manipulation evaluations with several SOTA methods published in the past three years.

**Cross-Datasets Evaluations** The cross-datasets evaluation is still a challenging task because the unknown domain gap between the training and testing datasets can be

caused by different source data, forgery methods, and/or post-processing. In this part, we evaluate the generalization performances in a cross-dataset setting. Specifically, our models were trained on the FF++ (only containing DF, F2F, FS, and NT subsets for fair comparisons) and tested on other datasets. Our method is compared with several state-of-the-art (SOTA) methods published in the past three years, including: UiA-ViT(Zhuang et al. 2022), DCL(Sun et al. 2022), CFM (Luo et al. 2023), AUNet(Bai et al. 2023), SLADD(Chen et al. 2022), SBI(Shiohara and Yamasaki 2022), FoCus(Tian et al. 2024), UCF(Yan et al. 2023), TALL++(Xu et al. 2024), TALL(Xu et al. 2023), (Ba et al. 2024), SeeABLE(Larue et al. 2023), LSDA(Yan et al. 2024), LAA-Net(Nguyen et al. 2024), VLFFD(Sun et al. 2023), IID(Huang et al. 2023), SA3WT(Li et al. 2024), and Bi-LIG(Jiang et al. 2024). The experimental results in terms of frame-level and video-level AUC are shown in Table 2. Aside from its moderate performance on the CDF dataset, our method outperforms most competitors on the Wild, DFDC, and DFDCP datasets, which are closer to real-world scenarios. We also report the results trained on FF++/DF, and found our method still performs better than all the competitors on the Wild, DFDC, and DFDCP datasets. It is important to highlight that all competitors re-train backbone networks (e.g., ResNet18 and ViT), which consist of at least 10M trainable parameters. In contrast, our method utilizes a mere 0.078M parameters, illustrating that it can achieve superior general performance with fewer learnable parameters.

**Cross-Manipulations Evaluations** Existing face forgery detectors often struggle to handle emerging manipulation techniques. In this part, we conduct cross-manipulation experiments involving five forgery techniques, i.e., Deepfakes (DF), Face2Face (F2F), FaceSwap (FS), and NeuralTextures (NT), FaceShifterFSh. We examine models trained on one manipulation type and tested across the other three. As shown in Table 3, we can observe that our method can improve cross-manipulation performances. Note that for the face reenactment (i.e., F2F and NT), face identity is not changed, thus the performance is a little worse than SOTA.

Therefore, Face ID plays a limited guiding role, which leads to limited improvement of our method. These results highlight the effectiveness of our method in combating emerging unseen forgery methods.

### Evaluations of RepDFD

In this part, we perform several evaluations to explore the effectiveness of ReDFD. The main results of the following experiments are cross-datasets performances trained on FF++/DF.

**Impact of reprogramming paradigm** In this part, we evaluate the effectiveness of our reprogramming paradigm compared with other tuning paradigms. Specifically, for the fine-tuning of the image feature encoder  $E_I$ , two established methods were assessed: Full Fine-Tuning (FFT), entailing the adjustment of all parameters within  $E_I$ , and Linear Probing (LP), which incorporates a learnable linear layer while maintaining  $E_I$  as frozen. In addition, we reference a very recent work MoE-FFD(Kong et al. 2024), which presents a deepfake detection method jointly utilizing the LoRA and Adapter paradigms to tune a frozen  $E_I$ .

Beyond the image feature extractor-related tuning paradigms, our study also incorporated a text feature extractor-related tuning paradigm, CoOp(Zhou et al. 2022), into the comparison. This method maintains the CLIP frozen while introducing learnable text prompts to adapt CLIP for specific target tasks. As shown in Table 4, our approach outperforms other methods in most scenarios. LP and CoOp inadequately facilitate the transfer of the base CLIP model to the deepfake detection task, resulting in suboptimal generalization performance. We think that these two paradigms exhibit a shared issue; they influence the utilization of image features, rather than the extraction of these features. Compared with them, FFT, MoE-FFD, and ours can directly impact image feature extraction, consequently improving general performance across multiple datasets. Furthermore, our method achieves superior generalization using significantly fewer parameters. We speculate that utilizing a limited number of parameters to fit deepfake-related knowledge potentially preserves the generalization capabilities of the base model. Notably, the performance gain is substantial when using a larger CLIP model with our method. Conversely, the performance of MoE-FFD significantly declines when utilizing a larger model, suggesting possible overfitting. It reveals the potential of our approach to be effectively scaled to larger models.

**Impact of different text prompts** In this part, we investigate the effects of various text prompt configurations on RepDFD, encompassing fixed text prompts, randomly initialized text prompts, and our adaptive face-related text prompts (termed *dynamic text prompts*). It can be concluded from the experiment that the dynamic text prompts are more effective than the fixed those. We consider all groups of the real/fake text templates in Table 1, i.e.,  $\{T_0, T_1\}$ ,  $\{T_2, T_1\}$ ,  $\{T_2, T_3\}$ . Furthermore, we consider a special text prompt setting, named ‘Rand Text’, which contains two completely random initialized and frozen text embedding as long as the ‘Fixed Text’ ( $\{T_0, T_1\}$ ). As

| Model | Method      | # Para | CDF          | Wild         | DFDCP        | Avg          |
|-------|-------------|--------|--------------|--------------|--------------|--------------|
| ViT-L | FFT         | 303M   | 83.12        | 70.20        | 90.58        | 81.30        |
|       | LP          | 0.002M | 75.78        | 74.33        | 76.73        | 75.62        |
|       | MoE         | 41.34M | 86.21        | 80.00        | 77.51        | 81.24        |
|       | CoOp        | 0.057M | 74.72        | 74.07        | 75.82        | 74.87        |
|       | <b>Ours</b> | 0.078M | <b>89.94</b> | <b>88.05</b> | <b>95.03</b> | <b>91.01</b> |
| ViT-B | FFT         | 86M    | 79.64        | 66.84        | 89.86        | 78.78        |
|       | LP          | 0.001M | 61.96        | 68.81        | 76.91        | 69.23        |
|       | MoE         | 15.51M | <b>91.28</b> | <b>83.91</b> | 84.97        | 86.72        |
|       | CoOp        | 0.038M | 67.43        | 64.47        | 76.05        | 69.32        |
|       | <b>Ours</b> | 0.078M | 86.81        | 81.53        | <b>91.93</b> | <b>86.76</b> |

Table 4: Comparison of AUC (%) across different tuning paradigms in a cross-dataset setting. Results for MoE correspond to MoE-FFD and are sourced from the original publication. The ‘Avg’ column denotes the mean AUC computed over various datasets

| Method                | CDF          | Wild         | DFDCP        |
|-----------------------|--------------|--------------|--------------|
| Rand Text             | 82.46        | 82.30        | 89.00        |
| $\{T_0, T_1\}$        | 82.88        | 84.91        | 88.62        |
| $\{T_2, T_3\}$        | 85.98        | 80.85        | 87.28        |
| $\{T_2, T_1\}$        | 85.26        | 84.80        | 87.38        |
| $\{T_0, T_3\}$ (Ours) | <b>88.41</b> | <b>87.73</b> | <b>90.68</b> |

Table 5: Comparisons of AUC (%) across different text prompt configurations in a cross-dataset setting. These models were trained on FF++ (DF)

shown in Table 5, the best performance occurred when the face embeddings are only utilized in the text prompt for the fake class, corresponding to the dynamic text prompts setting  $\{T_0, T_3\}$ . We observed that the ‘Fixed Text’ ( $\{T_0, T_1\}$ ) demonstrated limited effectiveness, performing similarly to ‘Rand Text’, which lacks substantive semantic content. This observation implies that semantic content in language may not significantly influence deepfake detection tasks, as the focus primarily lies on trace analysis. In contrast, integrating face embeddings into text prompts to create dynamic text prompts, corresponding to  $\{T_2, T_3\}$ ,  $\{T_2, T_1\}$ ,  $\{T_0, T_3\}$ , boosted model performance. We posit that the operation introduces fine-grained and face-related visual information into text prompts, thereby incorporating details that are challenging to describe linguistically. Therefore, the dynamic text prompts can not only enrich the supervision information during training, but also provide sample-level adaptive information to support classification.

**Impact for different face embeddings** To further verify the universality of Face2Text, we investigate the impact of different face embeddings on Face2Text prompts. We perform an ablation study comparing the results obtained by ArcFace(Deng et al. 2019), BlendFace(Shiohara, Yang, and Taketomi 2023) and Transface(Dan et al. 2023) and non-face (i.e., using the text prompt group  $\{T_0, T_1\}$ ). As shown in



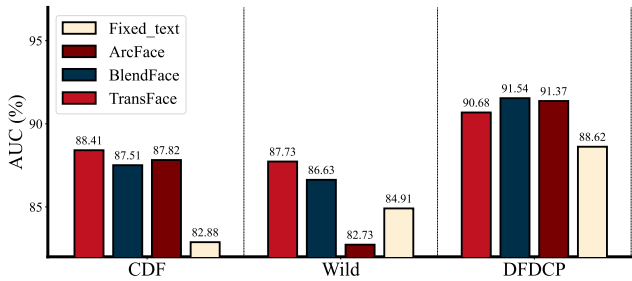


Figure 5: Comparisons of AUC (%) of our method incorporating with various face embeddings.

| Data | $T_0$  | $T_1$  | $T_2$  | $T_3$  |
|------|--------|--------|--------|--------|
| FF++ | 0.1889 | 0.1989 | 0.1757 | 0.2053 |
| CDF  | 0.1996 | 0.2002 | 0.1851 | 0.2021 |

Table 6: The cosine similarity calculated between image features and various configurations of text prompts.

Figure 5, our method demonstrates good performance across various face encoders  $F_{id}$ .

## Discussion

In this subsection, we present several in-depth analyses below, aiming to better understand the effectiveness of our method.

**Why are asymmetric text prompts effective?** In Table 5, it is noteworthy that optimal performance is achieved when the  $\{T_0, T_3\}$  configuration is selected, which solely incorporates face embedding into the text for the fake label. To investigate the reason, as shown in Table 6, we calculated the cosine similarity between the image features extracted by the initialized visual prompt  $\delta$  and the text prompts, both with and without face embedding. Our findings indicate that cosine similarities tend to be higher for the real label ( $T_0$ ) when using the text prompt without face embeddings, and for the fake label ( $T_3$ ) when using the text prompt with face embeddings. We guess that text prompts with higher cosine similarities offer a better initialization for the CLIP model, enabling more effective fine-tuning of target models. This observation may benefit future methodological design.

**The visualization of feature distribution** In this experiment, we provide the visualization of feature distributions as shown in Figure 6. The influence of the visual prompt  $\delta$  is limited exclusively to the input images and not the models, ensuring that the image features can occupy in a consistent feature latent space. Initial observations suggest that there are significant differences in the original feature distributions between the CDF and FF datasets, which indicates the intrinsic domain discrimination capability of the unmodified CLIP. Moreover, before integrating visual prompts, the original CLIP model failed to differentiate between real and fake images. In contrast, within the FF dataset, real and fake images can be efficiently discriminated by equipping

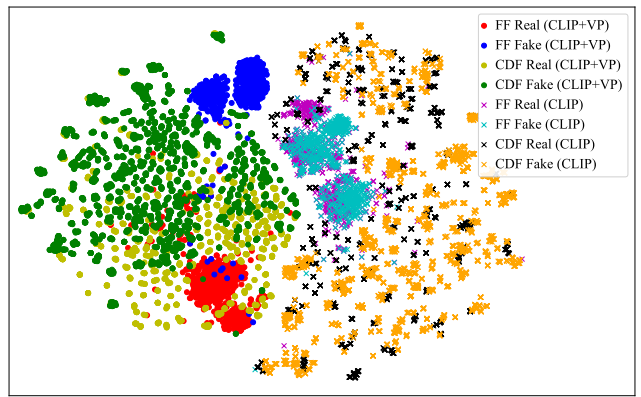


Figure 6: The t-SNE visualization of image features. 'CLIP' denotes features extracted by the original CLIP feature encoder, while 'CLIP+VP' refers to features extracted by the visual prompt.

visual prompts, suggesting the effectiveness of our method. Furthermore, although the CDF dataset was not used during training, visual prompts trained on the FF dataset effectively endowed the model with the capability to detect deepfakes in the CDF dataset. We speculate that the visual prompts  $\delta$ , consisting of a limited number of adjustable parameters, potentially tend to exploit the inherent capabilities of frozen models instead of introducing additional deepfake-information directly, which maybe protect the generalization ability of pretrained models so that improve the performance. We think the speculation is necessary to further explore in future works.

## Conclusions and Discussions

In this paper, we propose RepDFD, a general yet parameter-efficient method for detecting face forgeries by reprogramming a well-trained CLIP model. Specifically, we employ an Input Transformation technique to merge the image with learnable perturbations before feeding it into the CLIP image encoder. Additionally, we introduce Face2Text Prompts to incorporate facial identity information into the text prompts, which are then fed into the CLIP text encoder to guide the optimization of perturbations. The only required operation for evaluation is to apply these task-specific perturbations to all test images and then feed them into the CLIP model. Comprehensive experiments show that: (1) the cross-dataset and cross-manipulation performances of deepfake detection can be significantly and consistently improved using a pre-trained CLIP model with RepDFD; (2) our superior performances are at less cost of trainable parameters, making it a promising approach for real-world applications.

## References

An, X.; Deng, J.; Guo, J.; Feng, Z.; Zhu, X.; Yang, J.; and Liu, T. 2022. Killing two birds with one stone: Efficient and robust training of face recognition cnns by partial fc. In *Proceedings of the IEEE/CVF conference on computer vision and pattern recognition*, 4042–4051.

- Ba, Z.; Liu, Q.; Liu, Z.; Wu, S.; Lin, F.; Lu, L.; and Ren, K. 2024. Exposing the deception: Uncovering more forgery clues for deepfake detection. In *Proceedings of the AAAI Conference on Artificial Intelligence*, volume 38, 719–728.
- Bahng, H.; Jahanian, A.; Sankaranarayanan, S.; and Isola, P. 2022. Exploring Visual Prompts for Adapting Large-Scale Models. [arXiv:2203.17274](https://arxiv.org/abs/2203.17274).
- Bai, W.; Liu, Y.; Zhang, Z.; Li, B.; and Hu, W. 2023. Aunet: Learning relations between action units for face forgery detection. In *Proceedings of the IEEE/CVF Conference on Computer Vision and Pattern Recognition*, 24709–24719.
- Bordes, F.; Pang, R. Y.; Ajay, A.; Li, A. C.; Bardes, A.; Petryk, S.; Mañas, O.; Lin, Z.; Mahmoud, A.; Jayaraman, B.; Ibrahim, M.; Hall, M.; Xiong, Y.; Lebensold, J.; Ross, C.; Jayakumar, S.; Guo, C.; Bouchacourt, D.; Al-Tahan, H.; Padthe, K.; Sharma, V.; Xu, H.; Tan, X. E.; Richards, M.; Lavoie, S.; Astolfi, P.; Hemmat, R. A.; Chen, J.; Tirumala, K.; Assouel, R.; Moayeri, M.; Talattof, A.; Chaudhuri, K.; Liu, Z.; Chen, X.; Garrido, Q.; Ullrich, K.; Agrawal, A.; Saenko, K.; Celikyilmaz, A.; and Chandra, V. 2024. An Introduction to Vision-Language Modeling.
- Chen, L.; Zhang, Y.; Song, Y.; Liu, L.; and Wang, J. 2022. Self-supervised learning of adversarial example: Towards good generalizations for deepfake detection. In *Proceedings of the IEEE/CVF conference on computer vision and pattern recognition*, 18710–18719.
- Chen, P.-Y. 2024. Model Reprogramming: Resource-Efficient Cross-Domain Machine Learning. *Proceedings of the AAAI Conference on Artificial Intelligence*, 38(20): 22584–22591.
- Chen, X.; Ni, B.; Liu, Y.; Liu, N.; Zeng, Z.; and Wang, H. 2024. SimSwap++: Towards Faster and High-Quality Identity Swapping. *IEEE Transactions on Pattern Analysis and Machine Intelligence*, 46(1): 576–592.
- Chollet, F. 2017. Xception: Deep Learning With Depthwise Separable Convolutions. In *Proceedings of the IEEE Conference on Computer Vision and Pattern Recognition*, 1251–1258.
- Cozzolino, D.; Poggi, G.; Corvi, R.; Nießner, M.; and Verdoliva, L. 2024. Raising the Bar of AI-generated Image Detection with CLIP. In *Proceedings of the IEEE/CVF Conference on Computer Vision and Pattern Recognition Workshops*, 4356–4366.
- Dan, J.; Liu, Y.; Xie, H.; Deng, J.; Xie, H.; Xie, X.; and Sun, B. 2023. TransFace: Calibrating Transformer Training for Face Recognition from a Data-Centric Perspective. In *Proceedings of the IEEE/CVF International Conference on Computer Vision*, 20642–20653.
- Deng, J.; Guo, J.; Xue, N.; and Zafeiriou, S. 2019. ArcFace: Additive Angular Margin Loss for Deep Face Recognition. In *Proceedings of the IEEE/CVF Conference on Computer Vision and Pattern Recognition*, 4690–4699.
- Dolhansky, B.; Bitton, J.; Pflaum, B.; Lu, J.; Howes, R.; Wang, M.; and Ferrer, C. C. 2020. The DeepFake Detection Challenge (DFDC) Dataset. [arXiv:2006.07397 \[cs\]](https://arxiv.org/abs/2006.07397).
- Dolhansky, B.; Howes, R.; Pflaum, B.; Baram, N.; and Ferrer, C. C. 2019. The Deepfake Detection Challenge (DFDC) Preview Dataset. [arXiv:1910.08854 \[cs\]](https://arxiv.org/abs/1910.08854).
- Dosovitskiy, A.; Beyer, L.; Kolesnikov, A.; Weissenborn, D.; Zhai, X.; Unterthiner, T.; Dehghani, M.; Minderer, M.; Heigold, G.; Gelly, S.; Uszkoreit, J.; and Houshly, N. 2021. An Image Is Worth 16x16 Words: Transformers for Image Recognition at Scale. In *International Conference on Learning Representations*.
- Elsayed, G. F.; Goodfellow, I.; and Sohl-Dickstein, J. 2019. Adversarial Reprogramming of Neural Networks. In *International Conference on Learning Representations*.
- Huang, B.; Wang, Z.; Yang, J.; Ai, J.; Zou, Q.; Wang, Q.; and Ye, D. 2023. Implicit identity driven deepfake face swapping detection. In *Proceedings of the IEEE/CVF conference on computer vision and pattern recognition*, 4490–4499.
- Ilharc, G.; Wortsman, M.; Wightman, R.; Gordon, C.; Carlini, N.; Taori, R.; Dave, A.; Shankar, V.; Namkoong, H.; Miller, J.; Hajishirzi, H.; Farhadi, A.; and Schmidt, L. 2021. OpenCLIP.
- Jiang, P.; Xie, H.; Yu, L.; Jin, G.; and Zhang, Y. 2024. Exploring Bi-Level Inconsistency via Blended Images for Generalizable Face Forgery Detection. *IEEE Transactions on Information Forensics and Security*.
- Kong, C.; Luo, A.; Bao, P.; Yu, Y.; Li, H.; Zheng, Z.; Wang, S.; and Kot, A. C. 2024. MoE-FFD: Mixture of Experts for Generalized and Parameter-Efficient Face Forgery Detection.
- Larue, N.; Vu, N.-S.; Struc, V.; Peer, P.; and Christophides, V. 2023. SeeABLE: Soft Discrepancies and Bounded Contrastive Learning for Exposing Deepfakes. In *Proceedings of the IEEE/CVF International Conference on Computer Vision*, 21011–21021.
- Li, L.; Bao, J.; Yang, H.; Chen, D.; and Wen, F. 2020a. Advancing High Fidelity Identity Swapping for Forgery Detection. In *Proceedings of the IEEE/CVF Conference on Computer Vision and Pattern Recognition*, 5074–5083.
- Li, L.; Bao, J.; Zhang, T.; Yang, H.; Chen, D.; Wen, F.; and Guo, B. 2020b. Face X-Ray for More General Face Forgery Detection. In *Proceedings of the IEEE/CVF Conference on Computer Vision and Pattern Recognition*, 5001–5010.
- Li, Y.; Yang, X.; Sun, P.; Qi, H.; and Lyu, S. 2020c. Celeb-DF: A Large-Scale Challenging Dataset for Deep-Fake Forensics. In *Proceedings of the IEEE/CVF Conference on Computer Vision and Pattern Recognition*, 3207–3216.
- Li, Y.; Zhang, Y.; Yang, H.; Chen, B.; and Huang, D. 2024. SA 3 WT: Adaptive Wavelet-Based Transformer with Self-Paced Auto Augmentation for Face Forgery Detection. *International Journal of Computer Vision*, 1–23.
- Liu, H.; Li, X.; Zhou, W.; Chen, Y.; He, Y.; Xue, H.; Zhang, W.; and Yu, N. 2021. Spatial-Phase Shallow Learning: Rethinking Face Forgery Detection in Frequency Domain. In *Proceedings of the IEEE/CVF Conference on Computer Vision and Pattern Recognition*, 772–781.



- Luo, A.; Kong, C.; Huang, J.; Hu, Y.; Kang, X.; and Kot, A. C. 2023. Beyond the prior forgery knowledge: Mining critical clues for general face forgery detection. *IEEE Transactions on Information Forensics and Security*, 19: 1168–1182.
- Nguyen, D.; Mejri, N.; Singh, I. P.; Kuleshova, P.; Astrid, M.; Kacem, A.; Ghorbel, E.; and Aouada, D. 2024. LAA-Net: Localized Artifact Attention Network for Quality-Agnostic and Generalizable Deepfake Detection. In *Proceedings of the IEEE/CVF Conference on Computer Vision and Pattern Recognition*, 17395–17405.
- Ojha, U.; Li, Y.; and Lee, Y. J. 2023. Towards Universal Fake Image Detectors That Generalize Across Generative Models. In *Proceedings of the IEEE/CVF Conference on Computer Vision and Pattern Recognition*, 24480–24489.
- Qian, Y.; Yin, G.; Sheng, L.; Chen, Z.; and Shao, J. 2020. Thinking in Frequency: Face Forgery Detection by Mining Frequency-Aware Clues. In *ECCV*, 86–103.
- Radford, A.; Kim, J. W.; Hallacy, C.; Ramesh, A.; Goh, G.; Agarwal, S.; Sastry, G.; Askell, A.; Mishkin, P.; Clark, J.; Krueger, G.; and Sutskever, I. 2021. Learning Transferable Visual Models From Natural Language Supervision. In *Proceedings of the 38th International Conference on Machine Learning*, 8748–8763. PMLR.
- Rossler, A.; Cozzolino, D.; Verdoliva, L.; Riess, C.; Thies, J.; and Niessner, M. 2019. FaceForensics++: Learning to Detect Manipulated Facial Images. In *Proceedings of the IEEE/CVF International Conference on Computer Vision*, 1–11.
- Sha, Z.; Li, Z.; Yu, N.; and Zhang, Y. 2023. DE-FAKE: Detection and Attribution of Fake Images Generated by Text-to-Image Generation Models. In *Proceedings of the 2023 ACM SIGSAC Conference on Computer and Communications Security*, 3418–3432.
- Shiohara, K.; and Yamasaki, T. 2022. Detecting Deepfakes With Self-Blended Images. In *Proceedings of the IEEE/CVF Conference on Computer Vision and Pattern Recognition*, 18720–18729.
- Shiohara, K.; Yang, X.; and Taketomi, T. 2023. Blendface: Re-designing identity encoders for face-swapping. In *Proceedings of the IEEE/CVF International Conference on Computer Vision*, 7634–7644.
- Sun, K.; Chen, S.; Yao, T.; Sun, X.; Ding, S.; and Ji, R. 2023. Towards General Visual-Linguistic Face Forgery Detection. arXiv:2307.16545.
- Sun, K.; Yao, T.; Chen, S.; Ding, S.; Li, J.; and Ji, R. 2022. Dual Contrastive Learning for General Face Forgery Detection. In *Proceedings of the AAAI Conference on Artificial Intelligence*, volume 36, 2316–2324.
- Tan, M.; and Le, Q. 2019. EfficientNet: Rethinking Model Scaling for Convolutional Neural Networks. In *International Conference on Machine Learning*, 6105–6114.
- Tian, J.; Chen, P.; Yu, C.; Fu, X.; Wang, X.; Dai, J.; and Han, J. 2024. Learning to Discover Forgery Cues for Face Forgery Detection. *IEEE Transactions on Information Forensics and Security*.
- Tsao, H.-A.; Hsiung, L.; Chen, P.-Y.; Liu, S.; and Ho, T.-Y. 2024. AutoVP: An Automated Visual Prompting Framework and Benchmark. In *The Twelfth International Conference on Learning Representations*.
- Xu, C.; Zhang, J.; Han, Y.; Tian, G.; Zeng, X.; Tai, Y.; Wang, Y.; Wang, C.; and Liu, Y. 2022. Designing One Unified Framework for High-Fidelity Face Reenactment and Swapping. In *Computer Vision – ECCV 2022*, 54–71.
- Xu, Y.; Liang, J.; Jia, G.; Yang, Z.; Zhang, Y.; and He, R. 2023. Tall: Thumbnail layout for deepfake video detection. In *Proceedings of the IEEE/CVF international conference on computer vision*, 22658–22668.
- Xu, Y.; Liang, J.; Sheng, L.; and Zhang, X.-Y. 2024. Learning Spatiotemporal Inconsistency via Thumbnail Layout for Face Deepfake Detection. *International Journal of Computer Vision*, 1–18.
- Yan, Z.; Luo, Y.; Lyu, S.; Liu, Q.; and Wu, B. 2024. Transcending forgery specificity with latent space augmentation for generalizable deepfake detection. In *Proceedings of the IEEE/CVF Conference on Computer Vision and Pattern Recognition*, 8984–8994.
- Yan, Z.; Zhang, Y.; Fan, Y.; and Wu, B. 2023. Ucf: Uncovering common features for generalizable deepfake detection. In *Proceedings of the IEEE/CVF International Conference on Computer Vision*, 22412–22423.
- Yao, G.; Yuan, Y.; Shao, T.; Li, S.; Liu, S.; Liu, Y.; Wang, M.; and Zhou, K. 2021. One-Shot Face Reenactment Using Appearance Adaptive Normalization. *Proceedings of the AAAI Conference on Artificial Intelligence*, 35(4): 3172–3180.
- Zhang, K.; Zhang, Z.; Li, Z.; and Qiao, Y. 2016. Joint face detection and alignment using multitask cascaded convolutional networks. *IEEE signal processing letters*, 23(10): 1499–1503.
- Zhao, H.; Zhou, W.; Chen, D.; Wei, T.; Zhang, W.; and Yu, N. 2021. Multi-Attentional Deepfake Detection. In *Proceedings of the IEEE/CVF Conference on Computer Vision and Pattern Recognition*, 2185–2194.
- Zhou, K.; Yang, J.; Loy, C. C.; and Liu, Z. 2022. Learning to Prompt for Vision-Language Models. *International Journal of Computer Vision*, 130(9): 2337–2348.
- Zhuang, W.; Chu, Q.; Tan, Z.; Liu, Q.; Yuan, H.; Miao, C.; Luo, Z.; and Yu, N. 2022. UIA-ViT: Unsupervised inconsistency-aware method based on vision transformer for face forgery detection. In *European conference on computer vision*, 391–407. Springer.
- Zi, B.; Chang, M.; Chen, J.; Ma, X.; and Jiang, Y.-G. 2020. WildDeepfake: A Challenging Real-World Dataset for Deepfake Detection. In *Proceedings of the 28th ACM International Conference on Multimedia*, 2382–2390.

We elaborate on more details and results of our work in this supplementary material.

## More Details of Settings

### More Implementation Details

Our method is implemented by PyTorch 2.0.1 on a workstation equipped with one NVIDIA L40 GPU (48GB memory) and the CUDA Version is 12.4.

In the pre-processing stage, for every video frame in datasets, we employed MTCNN(Zhang et al. 2016) to detect and crop the facial regions, enlarged by a factor of 1.3, and subsequently resized them to  $224 \times 224$ .

All of the code and pre-trained models of CLIP are stemmed from the official repository OpenCLIP(Ilharco et al. 2021). For extracting face embeddings, we employed Transface(Dan et al. 2023) as the default face encoder in our method, using ViT-L version pre-trained on Glint360K(An et al. 2022). It should be noticed that the dimension of face embeddings is 512. For CLIP-ViT-B, the face embedding can directly be integrated into text embeddings, due to the naturally alignment of dimension. For CLIP-ViT-L, the text embedding dimension is 768, which presents a feature integration mismatch issue. To address the issue, a random projection layer was implemented to project the face embeddings into the target dimension. The random projection layer was initialized using the function `nn.init.normal(mean=0, std=1/768)`.

During training, the training batch size was set to 32 and our method did not utilize any data augmentations.

### More Details of Datasets

We conduct evaluations on widely-used datasets and follow previous settings used in their corresponding datasets and compare with other methods respectively. More details on these datasets are described below.

- **CelebDF (CDF)** (Li et al. 2020c) contains 590 real videos of 59 celebrities and corresponding 5639 high-quality fake videos generated by an improved forgery method. We use the stand test set consisting of 518 videos for our experiments.
- **DeepFake Detection Challenge Preview (DFDCP)** (Dolhansky et al. 2019) is generated by two kinds of synthesis methods on 1131 original videos. We use all 5250 videos for our experiments.
- **DeepFake Detection Challenge (DFDC)** (Dolhansky et al. 2020) is widely acknowledged as the most challenging dataset due to containing many manipulation methods and perturbation noises. We use the public test set consisting of 5000 videos for our experiments.
- **WildDeepfake (Wild)** (Zi et al. 2020) contains 3805 real face sequences and 3509 fake face sequences collected from Internet. Thus, it has a variety of synthesis methods and backgrounds, as well as character identities. We use the stand test set consisting of 806 sequences for our experiments.

| $p$ | #Para   | CDF   | Wild  | DFDCP | Avg          |
|-----|---------|-------|-------|-------|--------------|
| 12  | 0.031 M | 85.28 | 85.25 | 89.82 | 86.78        |
| 23  | 0.055 M | 85.55 | 87.01 | 90.88 | 87.81        |
| 34  | 0.078 M | 88.41 | 87.73 | 90.68 | <b>88.94</b> |
| 45  | 0.097 M | 80.64 | 82.68 | 90.37 | 84.56        |
| 56  | 0.113 M | 82.17 | 85.99 | 91.40 | 86.49        |
| 67  | 0.126 M | 78.59 | 80.05 | 88.65 | 82.43        |
| 78  | 0.137 M | 74.18 | 70.10 | 86.90 | 77.06        |

Table 7: The generalization performance involves different  $p$  of the visual prompt. All models were trained on FF++ (DF).

### Impact of the Visual Prompt Size

In our method, we incorporate visual prompts with input images processed through Input Transformation. Thus, the border width  $p$  of visual prompts impacts both performance and the number of learnable parameters. Herein, we conducted an ablation study to explore the impact of  $p$  was varied among the values  $\{12, 23, 34, 45, 56, 67, 78\}$ . This variation corresponds to resizing the input images to  $\{90\%, 80\%, 70\%, 60\%, 50\%, 40\%, 30\%\}$  of their original size, and then pad it to original size by merging the visual prompt. Table 7 exhibits the impact of varying  $p$ . Intuitively, the learnable parameters of the visual prompt increase with an increase in  $p$ . However, it is worth noting that as  $p$  increases, the average generalization performances of the model initially improves but then drops significantly. We speculate that such decline can be attributed to information loss caused by excessive scaling down of the images, suggesting a necessary trade-off between learnable parameters and the size of the input images. Therefore, we set  $p = 34$  in our experiments, corresponding to a resized image that is 70% of its original size.